SPECIAL TOPIC — Physical research in liquid crystal

# Phase-only stereoscopic hologram calculation based on Gerchberg–Saxton iterative algorithm*

Xinyi Xia(夏心怡) and Jun Xia(夏军)†

*Display Center, School of Electronic Science and Engineering, Southeast University, Nanjing* 210096, *China*

(Received 16 May 2016; published online 19 July 2016)

A phase-only computer-generated holography (CGH) calculation method for stereoscopic holography is proposed in this paper. The two-dimensional (2D) perspective projection views of the three-dimensional (3D) object are generated by the computer graphics rendering techniques. Based on these views, a phase-only hologram is calculated by using the Gerchberg–Saxton (GS) iterative algorithm. Comparing with the non-iterative algorithm in the conventional stereoscopic holography, the proposed method improves the holographic image quality, especially for the phase-only hologram encoded from the complex distribution. Both simulation and optical experiment results demonstrate that our proposed method can give higher quality reconstruction comparing with the traditional method.

**Keywords:** phase retrieval, computer-generated holograms, holography

**PACS:** 42.30.Rx, 42.40.Jv, 42.40.–I **DOI:** 10.1088/1674-1056/25/9/094204

## 1. Introduction

The concept of computer-generated holography (CGH) was first proposed by Kozman and Kelly.[1] With the development of computer technology, there are three categories of methods developed for calculating CGH, which are the point source algorithm, the polygon-based method, and the stereoscopic hologram algorithm.[2]

As we know, a three-dimensional (3D) scene can be precisely described by a number of point sources. Based on this characteristic, Slinger and Cameron proposed an algorithm which divided the 3D object into multiple point sources, and the light field generated by each point source was superimposed to form the whole light field of the 3D scene.[3–5] However, for a complex 3D object, the huge number of point sources increased the computational complexity, so the calculation efficiency was very low.

3D objects can also be divided into multiple planar segments[6,7] Detlef Leseberg proposed a method to calculate a rotary transform for the complex amplitude in a Fourier domain, and the complex distribution of hologram was calculated by superimposing the diffraction waves from the inclined planes.[8,9] But he did not give the complete rotation transform formula and results. Based on the angular spectrum theory and the coordinate rotation in Fourier domain, Kyoji Matsushima proposed a new method to calculate the transmission processes of a light field.[10] The method applied a twice Fourier transform and a spectrum interpolation for each segment to obtain a hologram with a complex distribution. However, similar to a point source algorithm, a 3D object often has a large number of planar segments, thus real-time calculation becomes a big problem. Lukas Ahrenberg proposed a solution for this problem.[11] Based on the angular spectrum theory, Ahrenberg directly calculated the light field distribution of the hologram by using only once fast Fourier transform (FFT) in the frequency domain, thus avoiding FFT computation for every segment. However, the shading and occlusion effect still remains a problem for this method. Hwi Kim solved the occlusion problem by the ray casting and ray tracing techniques.[12] Nonetheless, the heavy computational loads of the ray-object processes brought in the problem of calculation speed again.

In this paper, we focus on the stereoscopic hologram algorithm. King *et al.*[1] proposed to use a computer to calculate and store the perspective projection images of the 3D subject from several viewpoints and then recorded them on microfilms. The hologram can be generated through the interference of the reference beam and the light field of each projection. Based on this method, Toyohiko Yatagai proposed a new way to reconstruct 3D scenes.[13] After getting the perspective projection images of the 3D subject, the fast Fourier transform of each projection would be calculated to generate the corresponding sub-hologram by a computer. Then all sub-holograms would be tiled as a whole hologram according to the viewpoint order (i.e. stereoscopic hologram). According to the process of stereoscopic holography, the computational complexity is related to the number of viewpoints and the resolution of the sub-hologram, so the calculation speed could be promoted for real-time implementation. Computer graphics rendering techniques can be applied in stereogram

*Project supported by the National Basic Research Program of China (Grant No. 2013CB328803) and the National High Technology Research and Development Program of China (Grant Nos. 2013AA013904 and 2015AA016301).

†Corresponding author. E-mail: xiajun@seu.edu.cn

© 2016 Chinese Physical Society and IOP Publishing Ltd 

computations to add multiple shading effects and this will eventually make the 3D scene more realistic, so the occlusion problem can be automatically solved during the rendering processes.[14]

As the diffraction efficiency of the phase-only spatial light modulator (SLM) is very high, which is 100% in theory, it is widely used for holographic display.[15–17] Since it can only modulate the phase of the incident light, if we merely take the phase distribution of the hologram, the loss of amplitude information would bring errors in the reconstruction.[18,19] Our goal in this paper is to realize a method that can obtain the phase-only stereoscopic hologram with accurate reconstruction of 3D scenes.

The Gerchberg–Saxton (GS) iterative algorithm is a phase retrieval algorithm, which was first proposed by Gerschberg and Saxton in 1972.[20] It has been widely used in CGH because of the high accuracy of the reconstructed phase information. But it can only be used for two-dimensional (or one-dimensional) signals, so it is commonly applied in the projection of 2D images or 3D scenes consisting of multiple 2D planes which introduces a propagation process between each plane and still leaves the shading and occlusion a big problem.[21–23] Our proposed method takes the GS iterative algorithm instead of the non-iterative algorithm in the stereoscopic holography. On one hand, it can achieve a phase-only hologram with high precision; on the other hand, it can solve the problems of computing speed and shading or occlusion effects, and directly record the light field information of the whole 3D scenes, avoiding the process between 2D planes.

## 2. Proposed method for calculating a phase-only stereoscopic hologram

### 2.1. The generation of a sub-image

There are several methods to describe the light field distribution of a 3D scene. One is to get the 2D intensity and depth image as a description of the 3D scene, and another is to use a light-field camera, or camera array or micro lens array and imaging sensor to acquire 2D parallax views of the 3D scene, which is always employed in stereoscopic holography. In our proposed method, a micro lens array is used to obtain the 2D perspective projection views (sub-images) of the 3D object, which is based on perspective geometry projection.[24] These views are then recorded on the imaging sensor, as shown in Fig. 1(a). The focal length of the micro lens array is $f_{\mathrm{m}}$. The 3D subjects are set in front of the lens array with distance $d_1$, while the imaging sensor is set at the imaging position of the lens array with distance $d_2$, where $d_1$ and $d_2$ satisfy the imaging formula

$$\frac{1}{d_1}+\frac{1}{d_2}=\frac{1}{f_{\mathrm{m}}}. \tag{1}$$

To satisfy the perspective projection geometry, $d_1$ is usually far greater than $f_{\mathrm{m}}$, which means $d_2 \approx f_{\mathrm{m}}$.

### 2.2. The generation of a phase-only holographic stereogram

After getting the sub-images of the 3D object, the hogel is calculated with respect to each sub-image by using the GS iterative algorithm, which is described in detail in the dotted box of Fig. 1(b). First, the complex distribution of the holographic plane is gained by calculating the FFT of one sub-image. Then an amplitude constrain is applied on the holographic plane; namely, the amplitude factor is forced to unit value, and the phase factor remains unchanged. Second, the complex distribution of the imaging plane is obtained by calculating the inverse FFT (IFFT) of the updated complex distribution of the holographic plane. Then another amplitude

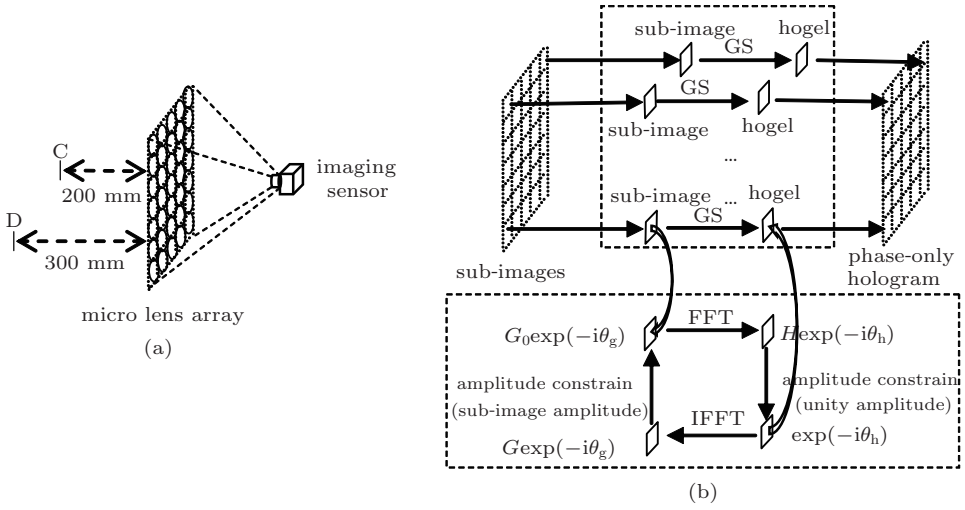



**Fig. 1.** Schematic diagrams of our proposed method: (a) the acquisition of sub-images, (b) the generation of final phase-only hologram.

constrain is applied on the image plane; namely, the amplitude factor is replaced by the amplitude value of the corresponding sub-image, and the phase factor remains unchanged. Next, the complex distribution of the holographic plane is generated by calculating FFT of the updated complex distribution of the imaging plane again. These steps are repeated until we have reached the correct number of iterations. Finally, the phase distribution generated in the iterative process is directly output as a one phase-only hogel.

After all of the hogels are calculated for the corresponding sub-images, they are eventually synthesized to a whole phase-only hologram according to the viewpoint order.

## 3. Experiment

In our experiment, the sub-images are generated by computer graphics rendering software, such as 3Dmax. The letters C and D are set up at the distances $Z_{\mathrm{C}} = 200$ mm and $Z_{\mathrm{D}} = 300$ mm from the micro lens array, respectively. The focal length of the micro lens array is $f_{\mathrm{m}} = 3.3$ mm and the diameter is $d = 0.4$ mm. The resolution of each sub-image is $120 \times 120$, and the number of the viewpoints is $16 \times 16$, which means that the final generated phase-only hologram contains $1920 \times 1920$ pixels.

### 3.1. Simulated experiment

#### 3.1.1. Calculation of sampling rate

As shown in Fig. 2, we take a point source as an example. The distance between the point and the lens is $d_1$, and the angle between the lights from the point to the center of the adjacent lens is $\theta$. The relationship of $d_1$ and $\theta$ is

$$\tan\theta = \frac{d}{d_1} \approx \sin\theta \approx \theta. \tag{2}$$

In the spectral domain, the variation of the frequency spectrum between the adjacent hogels is decided by the grating equation[18]

$$\Delta f_x = \frac{\sin\theta}{\lambda} = \frac{d}{\lambda d_1}, \tag{3}$$

where $\lambda$ is the wavelength of the light.

On the other hand, in the spatial domain, according to the theory of geometric similarity, we can figure out

$$\frac{d_1}{f_{\mathrm{m}}} = \frac{d}{\Delta x}, \tag{4}$$

where $\Delta x$ is the deviation of displacement in the spatial domain.

Let $N$ be the pixel number of the sub-image along the corresponding coordinate axis, the pixel interval $\Delta p$ on the sub-image is

$$\Delta p = \frac{d}{N}. \tag{5}$$

So the offset of the pixel number $m$ can be represented as

$$m = \frac{\Delta x}{\Delta p} = \frac{N f_{\mathrm{m}}}{d_1}. \tag{6}$$

Then back in the spectral domain, the sampling rate of the sub-image, namely, the spectrum of the hogel, is

$$\mathrm{d}f_x = \frac{\Delta f_x}{m} = \frac{d}{\lambda N f_{\mathrm{m}}}. \tag{7}$$

According to the sampling rate formula between the spectrum plane and the holographic plane, we can derive that the sampling rate of the hologram is

$$\mathrm{d}x = \frac{1}{N\,\mathrm{d}f_x} = \frac{\lambda f_{\mathrm{m}}}{d}. \tag{8}$$

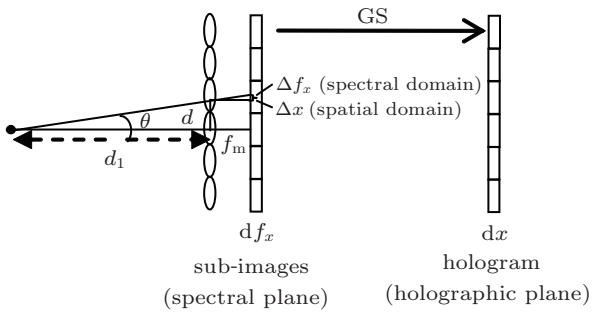



**Fig. 2.** Diagram of the sampling rate calculation, where $\theta$, $d$, $d_1$, $f_{\mathrm{m}}$, and $\Delta x$ are the parameters in the spatial domain, while $\Delta x$ and $\mathrm{d}f_x$ are the parameters in the spectral domain.

#### 3.1.2. Result

The simulation results of Fresnel reconstruction are shown in Fig. 3. The wavelength used for simulation is 532 nm. So according to Eq. (8), the calculated sampling rate of the hologram $\mathrm{d}x = 4.389$ μm . At one of the reconstructed planes with distance $Z_{\mathrm{C}} = 200$ mm, the letter C is focused whereas the letter D is out of focus, while at the other reconstructed plane of $Z_{\mathrm{D}} = 300$ mm, the situation is opposite. Figures 3(a) and 3(c) are the results of the traditional method in which the non-iterative algorithm with FFT is performed on each sub-image. We can see that the outline of the letters appears but the edge is not so clear and the content information is lost. Figures 3(b) and 3(d) show the results of our proposed method in which the number of GS iteration for each sub-image is 32 and it takes about 0.033 s. So the time for calculating the whole CGH by our algorithm is about 8.6 s. It is important to mention that all of the CGHs generated in the experiments are calculated by using a PC with a CPU of Intel(R) Core(TM) i7-5960X (3.00 GHz) and a memory of CORSAIR DDR4 (2666 MHz, 16 GB). Comparing Figs. 3(a) and 3(c) with Figs. 3(b) and 3(d), respectively, we find that after GS iteration, the letters turn out to be clearer in both the edges and the content area. The quality of the reconstructed images is improved remarkably by our proposed method.

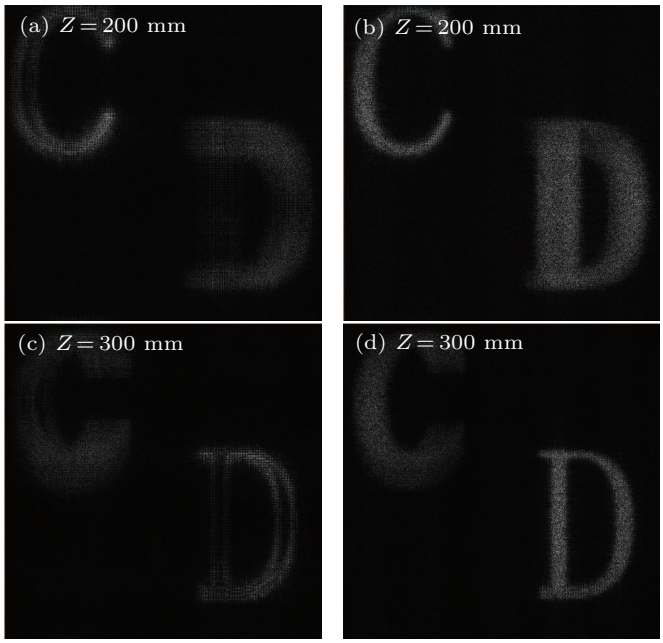



**Fig. 3.** Simulated results of letters C and D focused on the letter C ((a) traditional method, (b) the proposed method) and focused on the letter D ((c) traditional method, (d) the proposed method).

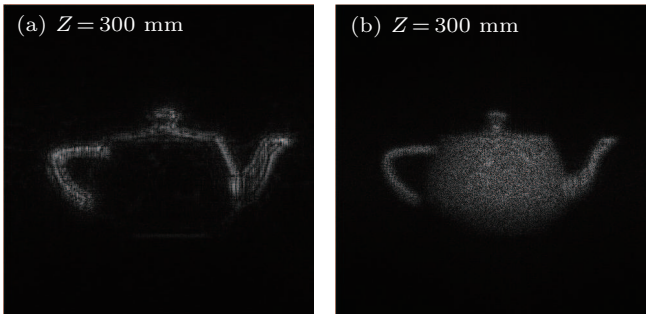



**Fig. 4.** Simulated results of the teapot: (a) traditional method, (b) the proposed method.

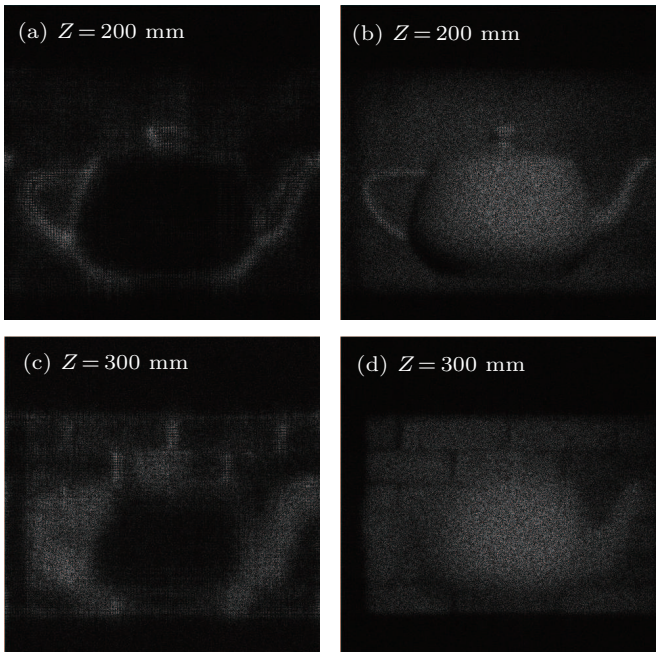



**Fig. 5.** Simulated results of the teapot and wall focused on the teapot ((a) traditional method, (b) the proposed method) and focused on the wall ((c) traditional method, (d) the proposed method).

The experiments of complex models, such as a teapot and a 3D scene which contains a teapot located at $Z_t = 200$ mm and a background wall located at $Z_w = 300$ mm, are also carried out and the results are shown in Figs. 4 and 5, respectively. In Fig. 4, we find that the missing information of the teapot is retrieved and the edges of the contour become clearer by our proposed method. Figures 5(a) and 5(b) are the reconstructed images focused on the teapot, and figures 5(c) and 5(d) are the reconstructed images focused on the wall. The reconstruction results by the traditional method are shown in Figs. 5(a) and 5(c), both of which miss some information because of the lack of amplitude distribution. Since the GS iterative algorithm is used in our proposed method, the reconstruction quality is improved. Moreover, we can see that the occlusion effect of the teapot and background wall is performed well.

### 3.2. Optical experiment

#### 3.2.1. Set up of the optical path

The light path diagram is presented in Fig. 6. The phase-only hologram is first loaded into the SLM by a computer. The 532 nm green laser beam first goes through a polarizer and is then reflected into the SLM by a beam splitter prism. After the light illuminates the screen of the SLM, the phase of each pixel is modulated, then the phase-modulated light continues to diffract in the optical system. The SLM used in our experiment is Holoeye with $1920 \times 1080$ pixels. The pixel pitch is 8 μm. Because of the discrete nature of the pixelated structure, the diffraction efficiency of Holoeye cannot reach to 100% but reaches around 60%. The central wavelength of Holoeye is consistent with the laser, so that the diffraction efficiency can reach its maximum. It is necessary to mention that the phase information of the spherical wave is added to the phase distribution of the hologram plane.[25] The reconstruction image would then be shifted from the focal plane of the Fourier lens and the unchanged zero-order illumination could be blocked by using a special filter.

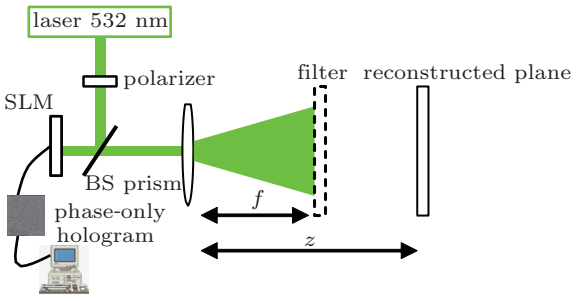



**Fig. 6.** (color online) Schematic diagram of the optical path.

#### 3.2.2. Result

Figures 7–9 show the results of the optical experiment. Figures 7(a)–7(d) are the results of the letters C and D corresponding to Figs. 3(a)–3(d), figures 8(a) and 8(b) are the

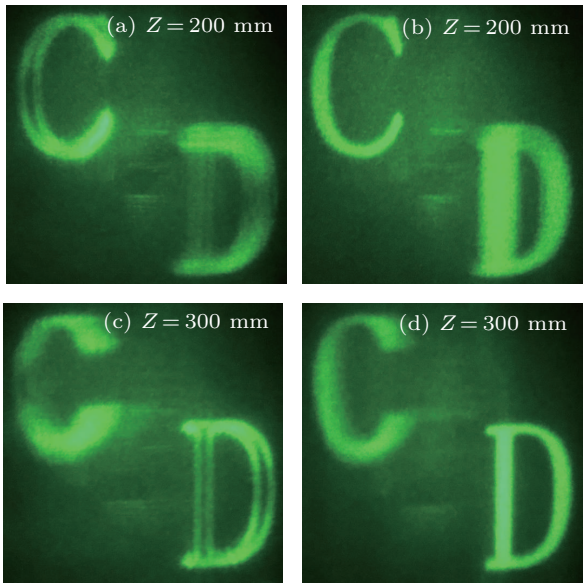



**Fig. 7.** (color online) Optical results of letters C and D focused on the letter C ((a) traditional method, (b) the proposed method) and focused on the letter D ((c) traditional method, (d) the proposed method).

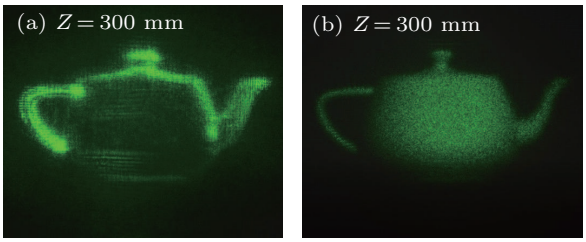



**Fig. 8.** (color online) Optical results of the teapot: (a) traditional method, (b) the proposed method.

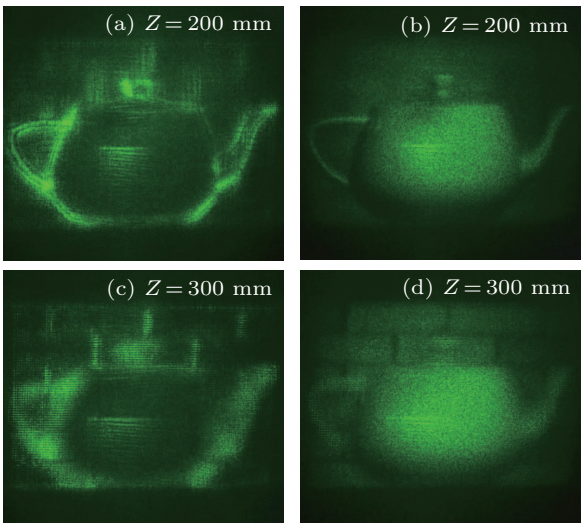



**Fig. 9.** (color online) Optical results of the teapot and wall focused on the teapot ((a) traditional method, (b) the proposed method) and focused on the wall ((c) traditional method, (d) the proposed method).

results of the teapot corresponding to Figs. 4(a) and 4(b), and figures 9(a)–9(d) are the results of the teapot and wall corresponding to Figs. 5(a)–5(d). It can be seen that the results of the optical experiment are consistent with those of the numerical simulation.

## 4. Conclusion

We propose a method to calculate phase-only CGH by using the GS iterative algorithm in stereoscopic holography. In contrast from the simple FFT processing of the traditional stereoscopic hologram calculation, the GS iterative algorithm is applied to the 2D perspective projection views of the 3D object (sub-images) to generate a phase-only hologram, which reduces the errors caused by missing the amplitude information so that the image information would be more complete. We also give the formula to calculate the sampling rate of the holographic plane. The simulated and optical experiments are conducted respectively. The results indicate that there is a significant improvement in the quality of the reconstructed image by our proposed method.

## References

[1] King M C, Noll A M and Berry D H 1970 *Appl. Opt.* **9** 471
[2] Ma J S, Xia F P and Su P 2012 *Opt. Precis. Eng.* **20** 1141 (in Chinese)
[3] Slinger C, Cameron C and Coomber S 2004 *Proc. SPIE* **5290** 27
[4] Slinger C, Cameron C and Stanley M 2005 *IEEE Computer* **38** 46
[5] Zhang X, Liu X and Chen X 2005 *International Society for Optics and Photonics* (Photonics Asia) p. 109
[6] Liu Y Z, Dong J W and Pu Y Y 2010 *Opt. Express* **18** 3345
[7] Liu Y Z, Dong J W and Pu Y Y 2011 *Opt. Lett.* **36** 2128
[8] Leseberg D and Frère C 1988 *Appl. Opt.* **27** 3010
[9] Leseberg D 1992 *Appl. Opt.* **31** 223
[10] Matsushima K, Schimmel H and Wyrowski F 2003 *JOSAA* **20** 1755
[11] Ahrenberg L, Benzie P and Magnor M 2008 *Appl. Opt.* **47** 1567
[12] Kim H, Hahn J and Lee B 2008 *Appl. Opt.* **47** D117
[13] Yatagai T 1976 *Appl. Opt.* **15** 2722
[14] Zhang H, Zhao Y and Cao L C 2015 *Opt. Express* **23** 3901
[15] Zhou Q, Lu J F and Yin J P 2013 *Chin. J. Liq. Cryst. Disp.* **28** 349
[16] Hu L F 2005 *Chin. J. Liq. Cryst. Disp* **20** 93 (in Chinese)
[17] Wu G Z, Zhang H S and Mao W Y 2014 *Chin. J. Liq. Cryst. Disp.* **29** 1010
[18] Kang H J, Yamaguchi T and Yoshikawa H 2008 *Appl. Opt.* **47** D44
[19] Zhao Y, Cao L C and Zhang H 2015 *Opt. Express* **23** 25440.
[20] Gerschberg R W and Saxton W O 1972 *Optik* **35** 237
[21] Qu W D, Gu H R and Zhang H 2015 *Appl. Opt.* **54** 10018
[22] Chang C L, Xia J and Lei W 2012 *Opt. Commun.* **285** 24
[23] Exarhos G J, Guenther A H and Kaiser N 2002 *34th Annual Boulder Damage Symposium on Optical Materials for High-Power Lasers/7th International Workshop on Laser Beam and Optics Characterization*, September 16–19, 2002, Natl Inst Stand & Technol, Boulder, Co, p. 590
[24] Park J H, Kim M S and Baasantseren G 2009 *Opt. Express* **17** 6320
[25] Zhang H, Xie J H and Liu J 2009 *Appl. Opt.* **48** 5834